

The Electroreductive Dechlorination Reaction of 2,3-Dichlorophenol on Pd/Ag/Cu

Fen Wang, Xian Jing Yang, Qi Guo Chen, Mei Chao Li*, Chun An Ma*

College of Chemical Engineering, Research Center of Analysis and Measurement, State Key Laboratory Breeding Base of Green Chemistry Synthesis Technology, Zhejiang University of Technology, Hangzhou 310032, China

*E-mail: limc@zjut.edu.cn (M.C. Li), science@zjut.edu.cn (C.A. Ma)

Received: 8 June 2015 / Accepted: 6 July 2015 / Published: 28 July 2015

Pd/Ag/Cu electrode was successfully prepared on Ag dendrites with Cu substrate (Ag/Cu) by galvanic replacement reactions, and was characterized by scanning electron microscopy, X-ray diffraction and transmission electron microscopy. The electroreductive dechlorination reaction of 2,3-dichlorophenol on Pd/Ag/Cu electrode was investigated by cyclic voltammetry and in situ FTIR techniques. Compared with Pd/Cu, Ag/Cu and Cu electrodes, Pd/Ag/Cu electrode exhibited the highest electrocatalytic activity for electroreductive reaction of 2,3-dichlorophenol. C-Cl bond was broken by reaction of adsorbed 2,3-dichlorophenolate with (H)_{ads}Pd on Pd/Ag/Cu electrode surface. The main intermediate was 2-chlorophenolate, and the final product was phenolate.

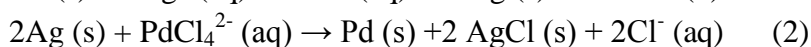
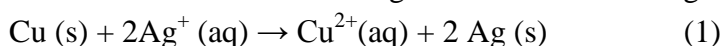
Keywords: Electroreductive dechlorination; 2,3-Dichlorophenols; Pd/Ag/Cu; In situ FTIR

1. INTRODUCTION

Chlorophenols have been extensively used for the synthesis of wood preservatives, dyes, pesticides and so on. During the manufacturing processes, they are introduced into the environment and can be found in ground waters and soils. Chlorophenols are toxic and resistant to biological degradation even at low concentrations, so they are listed as priority pollutants by United States Environmental Protection Agency (USEPA). Now the accumulation of chlorophenols in the environment has become a serious problem. Various techniques have been developed to treat them, such as biodegradation, chemical degradation, photocatalytic degradation and so on [1-3]. It is well known that chlorine-free organic compounds are usually much less toxic, and can be disposed by more convenient and economic manners [4]. Due to the simplicity in operation and mild reaction conditions

without secondary contaminants, electroreductive method has been proved to be one of the most attractive methods for dechlorination of chlorophenols [5,6].

In order to obtain good electrocatalytic efficiency, Pd nanoparticles obtained more and more attention due to the strong ability in adsorption of hydrogen. But nanoparticles are easy to aggregate into large particles during the preparation process, leading to deterioration of catalytic performance. To prepare Pd nanoparticles with high dispersion, some carbon materials or Al_2O_3 are used as the catalyst supports [7-10]. While Ag dendrites have a typical hierarchical structure with many side branches, and there are plenty of active atoms showing a high electrocatalytic activity and surface enhanced Raman scattering (SERS) [11-13]. Recently, Ag dendrites have even been used as the substrate to synthesis bimetallic particles, such as Ag/Au particles which show excellent catalytic activity for 4-nitrophenol reduction reaction [14]. Galvanic replacement reaction is an effective and simple method without complicated equipments and any additional reductive agents. In principle, the driving force for the galvanic replacement reaction is the equilibrium electrode potential difference between the deposited metal and the substrate. The following reactions occur during the galvanic replacement process:



Therefore, Ag dendrites on Cu substrate (Ag/Cu) can be obtained by the galvanic replacement reaction of AgNO_3 and Cu (Eq. (1)). Then, Pd particles are deposited onto the surface of Ag dendrites by a simple galvanic displacement reaction of Ag dendrites in H_2PdCl_4 solution (Eq. (2)) at room temperature (denoted as Pd/Ag/Cu). However, according to the literature survey, the researches about the electrocatalytic activity for electroreductive dechlorination of chlorophenols on Pd/Ag/Cu electrode are seldom reported.

As we know, the position of chlorine atom on the benzene ring will affect dechlorination sequence and electrochemical reaction mechanism of chlorophenols [15-17]. In this paper, 2,3-dichlorophenol (2,3-DCP) is chosen as the model molecule and Pd/Ag/Cu is chosen as the working electrode. Electrochemical in situ FTIR spectroscopy is a powerful technique to provide the change of reactants, intermediates and products on the surface of the electrode at given potentials directly [18]. Besides, density functional theory (DFT) calculation can be used to verify the experiment results, and the calculated results will supply theoretical guidance for electroreductive dechlorination reaction of 2,3-dichlorophenol. Therefore, the effect of chlorine position on the electroreductive dechlorination of 2,3-DCP on Pd/Ag/Cu electrode and its corresponding reaction mechanism are investigated by in situ FTIR technique together with DFT calculation.

2. EXPERIMENTAL

2.1 Preparation and characterization of Pd/Ag/Cu.

Prior to the preparation, Cu substrate was sequentially polished with 0.03-0.005 μm $\alpha\text{-Al}_2\text{O}_3$ powders, and then sonicated in acetone and dilute sulphuric acid, respectively. The clean Cu substrate was immersed into the deposition solution of AgNO_3 solution (5 mM) for 20 min, and Ag/Cu electrode

was obtained by galvanic replacement reaction of AgNO_3 and Cu. Then Ag/Cu electrode was immersed into the deposition solution of H_2PdCl_4 (2.5 mM) for 40 min to prepare Pd/Ag/Cu electrode. Finally, the Pd/Ag/Cu electrode was rinsed in ultrapure water and dried in air. All the experiments were performed at room temperature. For comparison, Pd/Cu was also prepared by the galvanic replacement reaction of H_2PdCl_4 and Cu.

The morphology was characterized by scanning electron microscopy (SEM, Hitachi S-4700) at an accelerating voltage of 15 kV. Transmission electron microscopy (TEM) was performed on a high resolution transmission electron microscope (FEI, Tecnai G2 F30 S-Twin) at an accelerating voltage of 300 kV. Pd/Ag particles on Pd/Ag/Cu were scraped from the Cu substrate. Then they were dispersed in ethanol ultrasonically and dropped on a nickel mounted holey carbon film. The powder X-ray diffraction patterns of Pd/Ag particles were performed on a X-ray diffractometer using Cu-K α radiation (Thermo SCINTAG X00 TRA, $\lambda=0.15418$ nm).

2.2 Electrochemical experiments

2,3-Dichlorophenol (98%) was purchased from Aladdin Reagent Co. Ltd. (Shanghai) and used without further purification. 1 M NaOH was used as the supporting electrolyte. All the solutions were prepared with ultrapure water supplied from Milli-Q system (Millipore, Japan). Cyclic voltammetric measurements were performed on CHI620B electrochemical workstation. (CH Instrument Inc.) A three-electrode cell with a saturated calomel electrode (SCE) and a Pt sheet (3 cm²) counter electrode was used. All potentials reported in this paper were referred to SCE.

The electrolysis experiments were performed in a two-compartment cell, divided by a cation-exchange membrane (Nafion 117), and assembled with magnetic stirring bar. The cathode was Pd/Ag/Cu cathode (2 cm \times 4 cm) and a graphite flake (2 cm \times 4 cm) was used as the anode. The electrolysis experiment was performed on laboratory direct current power in neutral solution containing 0.5 mM 2,3-DCP with the constant current 150 mA. The composition variation of the electrolytic processes was monitored by high performance liquid chromatography (HPLC) system equipped with a Waters 2996 Photodiode Array Detector.

2.3 In situ FTIR investigation.

The electrochemical measurements were performed on a EG&G potentiostat/galvanostat 263A and the in situ FTIR spectra were obtained with a Nicolet 670 FTIR spectrometer equipped with MCT-A detector cooled with liquid nitrogen. A spectroelectrochemical cell coupled to a CaF_2 disk window (32 mm \times 2 mm) was used for the in situ FTIR electro spectroscopic measurements. All normalized IR spectra obtained were calculated as $\Delta R/R$ according to the formula:

$$\Delta R/R = [R(E_S) - R(E_R)] / R(E_R) \quad (3)$$

$R(E_S)$ and $R(E_R)$ were the single-beam spectra of reflection measured at sample potential E_S and reference potential E_R , respectively [19,20]. According to Eq. (3), the negative-going bands indicated the gain of the intermediates or products in the thin layer solution, and positive-going bands

indicated the consumption of reactants. Each spectrum corresponded to 200 interferometer scans taken at 8 cm^{-1} resolution and the polarization time was about 90 s.

2.4 Computations details

The calculations were performed in the framework of DFT. In DFT computation of molecular orbital analyses, Becke's three parameter hybrid exchange functional combined with the Lee-Yang-Parr's correlation function (B3LYP) was accepted as a cost-effective approach for the computation of molecular structure [21-24]. DFT/B3LYP/6-311G++(d,p) was carried out to calculate the energy and geometry optimization, which were confirmed by frequency calculations to ensure that each of the geometries corresponded to a minimum on the potential energy surface. Bond dissociation energy (BDE) was an important parameter in the study of reaction mechanism. Based on BDE values, the dechlorination pathway could be predicted and the one with the lower bond energy can easily be separated [25]. The BDE values of C-Cl have been calculated according to the expression [26]:

$$DH^0(R-X) = \Delta_f H^0(R\cdot) + \Delta_f H^0(X\cdot) - \Delta_f H^0(R-X) \quad (4)$$

$\Delta_f H^0$ represented the heats of formation of the respective species in the ideal gas state at 1 atm. All the calculations are performed with the Gaussian03 package program.

3. RESULTS AND DISCUSSION

3.1 Characterization of Pd/Ag/Cu

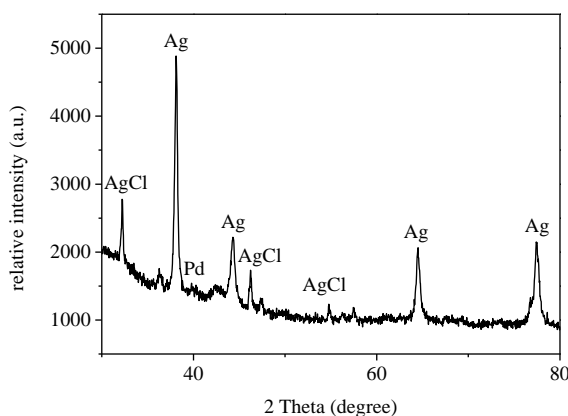


Figure 1. XRD pattern of the Pd/Ag/Cu particles.

The XRD pattern of Pd/Ag/Cu particles is illustrated in Fig. 1. Four diffraction peaks were indexed to characteristic diffractions from the (111), (200), (220) and (311) of cubic Ag (Card File, 03-065-2871). The (111) plane of Pd was observed at 40.8° . The absence of other peaks of Pd suggested that the crystalline lattice of Pd/Ag particles was dominated from Ag dendrites [27,28]. In addition, the other strong peaks ascribed to AgCl crystals were also observed (Card File, 00-001-1013), which were

formed during the galvanic displacement reaction between Ag particles and PdCl₄²⁻, as shown in Eq. (2). The existence of AgCl suggested that Pd particles were deposited on Ag/Cu successfully [28].

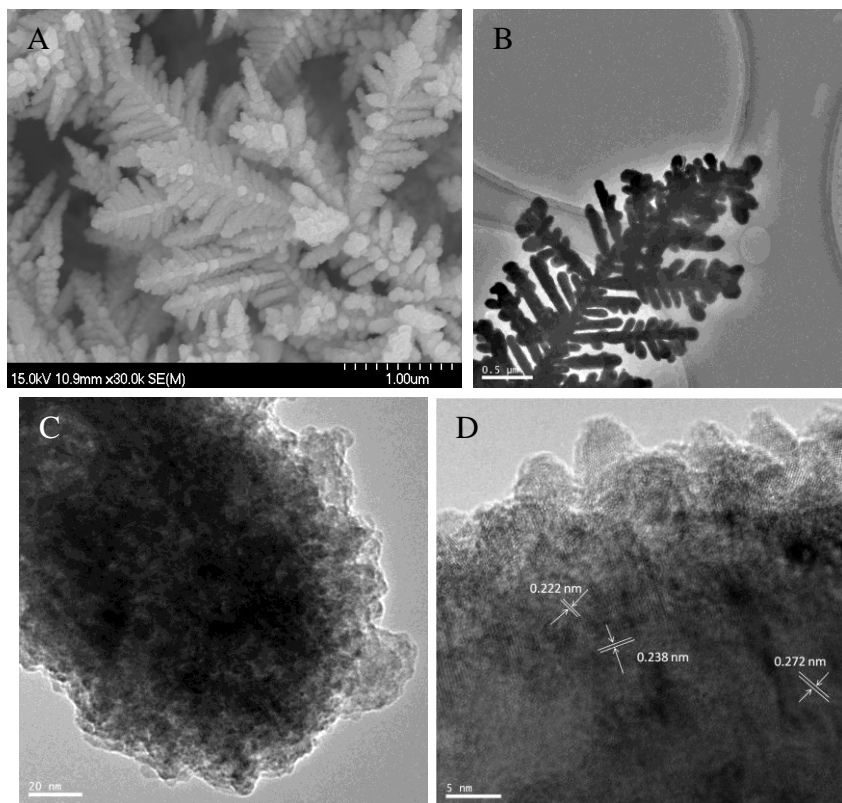
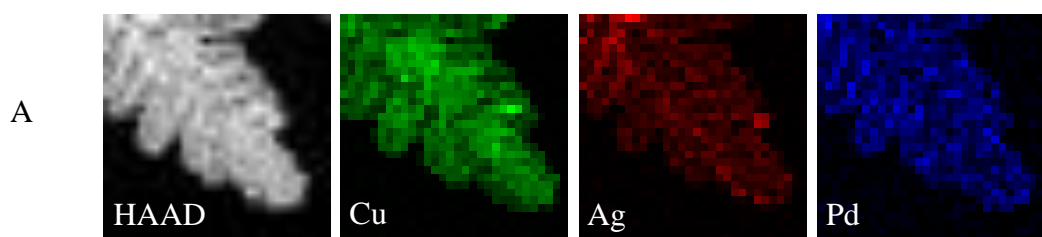


Figure 2. (A) SEM and (B) TEM images of Pd/Ag/Cu, (C) TEM and (D) HRTEM images of Pd/Ag/Cu branch tip.

Fig. 2A shows a SEM image of Pd/Ag/Cu dendrites. It consisted of a long central backbone with many branches which were columned. Dendritic structures were also displayed in the TEM images of Pd/Ag/Cu (Fig. 2B). The TEM and HRTEM images of subbranch tip of Pd/Ag/Cu dendrites are given in Fig. 2C and 2D. The surface and edge were rough and blurry. In addition, several different lattice fringes were observed in the the HRTEM image of Pd/Ag/Cu particles. The lattice fringe of 0.238 nm was related to the interplanar of Ag (111), the most stable crystal plane of Ag. Another two types of lattice fringes with interplanar spacings of 0.222 and 0.272 nm were ascribed to Pd (111) and AgCl (200), respectively. The results agreed well with XRD.



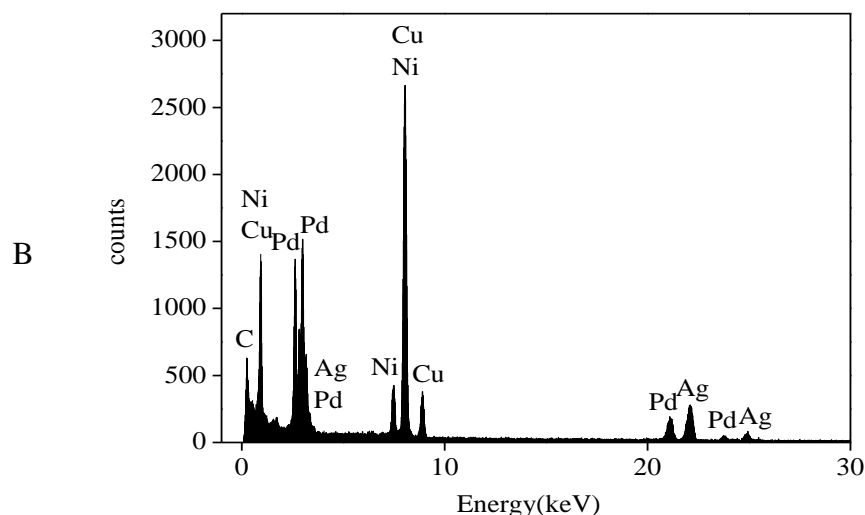


Figure 3. (A) HAADF-STEM and elemental mapping of Pd/Ag/Cu particles. (B) EDX spectrum of Pd/Ag/Cu particles.

3.2 Cyclic voltammetric characteristics of 2,3-DCP.

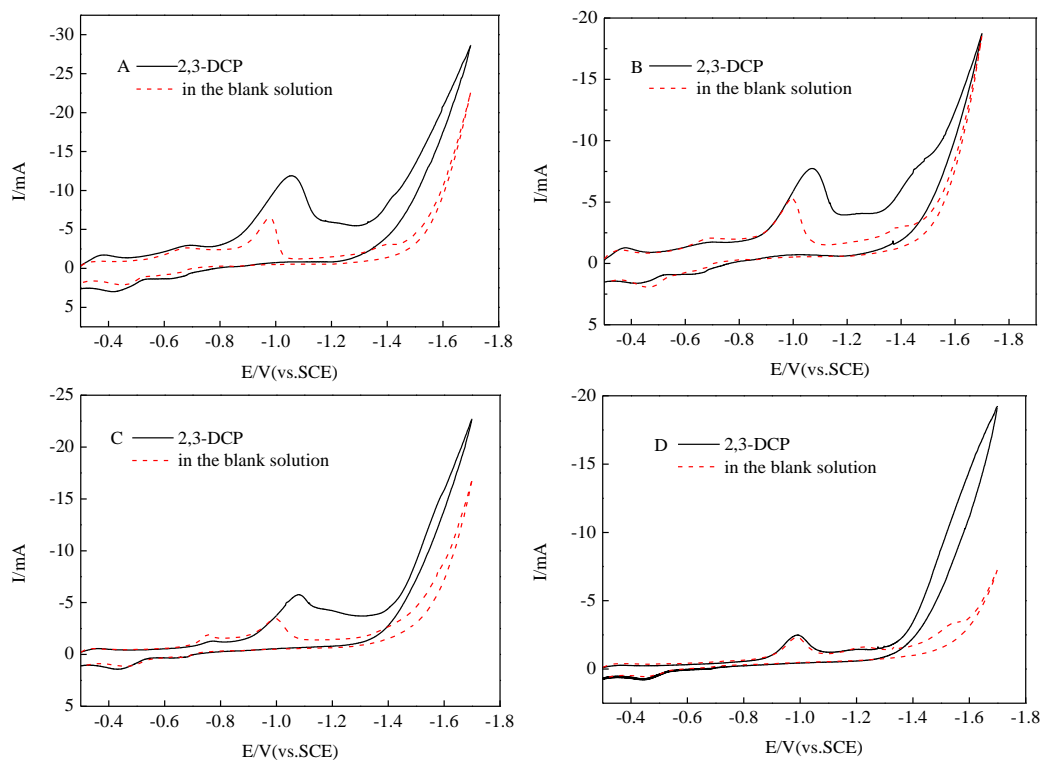


Figure 4. Cyclic voltammograms for the electroreduction of 2,3-DCP on different electrode surfaces: (A) Pd/Ag/Cu, (B) Pd/Cu, (C) Ag/Cu and (D) Cu.

Fig. 4A shows the cyclic voltammograms for the electroreductive reaction of 0.5 M 2,3-DCP on Pd/Ag/Cu electrode between -0.3 V and -1.7 V with the scan rate of $50 \text{ mV} \cdot \text{s}^{-1}$. Three reductive peaks at about -0.38 V, -0.69 V and -1.05 V could be seen in the blank solution (1 M NaOH) on

Pd/Ag/Cu electrode. According to the literatures, the reduction peak at -0.69 V was related to the electroreduction of water with the formation of adsorbed hydrogen on the surface of Pd/Ag/Cu electrode ($(\text{H})_{\text{ads}}\text{Pd}$). While the first peak was mainly originated from the reduction of palladium oxides, and the third peak was related to the reduction of copper oxides [29-31]. With the addition of 2,3-DCP into the blank solution, the third peak current became higher and broader, and was well evidenced with onset potential at about -0.80 V. Thus, there were other electrocatalytic reactions occurring on the Pd/Ag/Cu except from the reduction of copper oxides. It indicated that 2,3-DCP might be reduced on Pd/Ag/Cu electrode. There were no corresponding oxidation peaks of 2,3-DCP on the positive sweep, and the electroreductive dechlorination reaction of 2,3-DCP was irreversible.

For comparison, the electroreductive dechlorination reaction of 2,3-DCP on Pd/Cu, Ag/Cu and Cu electrodes were also investigated under the similar conditions respectively. The reductive peak current was -7.7 mA at about -1.08 V on Pd/Cu electrode, and the reduction peak current was -5.8 mA on Ag/Cu electrode. While the cyclic voltammogram showed no obvious change on the Cu electrode after adding 2,3-DCP in NaOH solution. As compared with Pd/Cu, Ag/Cu and Cu electrodes, the reductive current of electroreductive dechlorination reaction of 2,3-DCP on Pd/Ag/Cu electrode was highest, indicating that Ag dendrite-based Pd/Ag/Cu electrode showed the highest electrocatalytic activity for the reduction of 2,3-DCP.

3.3 In situ FTIR studies for the electroreductive dechlorination of 2,3-DCP on Pd/Ag/Cu electrode.

In situ FTIR spectra collected during the electroreductive reaction of 2,3-DCP in the spectral range of 1600-1000 cm^{-1} are shown in Fig. 5. At -300 mV, the spectra were dominated by five positive-going bands at 1570 and 1448 cm^{-1} (stretching vibration of benzene ring) [32], 1315 and 1257 cm^{-1} (C-O stretching vibration) and 1185 cm^{-1} (C-H in-plane bending vibration) [33,34]. Those bands were related to 2,3-dichlorophenolate species which were adsorbed on the surface of Pd/Ag/Cu electrode. Another strong and important positive-going band at 1045 cm^{-1} , which was assigned to stretching vibration of C2-Cl, generated from C2-Cl bond breakage. These positive-going bands mainly be due to the loss of 2,3-DCP in the thin layer solution between Pd/Ag/Cu disc electrode and CaF_2 window. As compared with the band of C2-Cl, the stretching vibration of C3-Cl was weak (about 930 cm^{-1}), and could not be observed in Fig. 5 because of CaF_2 window. It was noteworthy that there was an important negative-going band at 1122 cm^{-1} observed in Fig. 5, which pertained to C-H in plane bending vibration of adsorbed 2-chlorophenolate [35]. The above analysis could lead to the conclusion that electroreductive dechlorination reaction occurred from -300 mV to get the main intermediate 2-chlorophenolate with the consumption of adsorbed 2,3-dichlorophenolate.

In addition, the positive-going band at 1620 cm^{-1} was observed and related to the bending vibration of adsorbed water in the thin layer [36]. It was because that water was electrolyzed to generate hydrogen and adsorbed on the surface of Pd/Ag/Cu to form $(\text{H})_{\text{ads}}\text{Pd}$. With the potential stepping to more negative, most of the peak intensities increased and the negative-going bands were observed clearly, indicating that the electrochemical reaction of 2,3-DCP on the Pd/Ag/Cu electrode was more and more fierce.

At about -1100 mV, the well defined negative-going bands at 1581, 1515, 1481 and 1457 cm^{-1} were related to stretching vibrations of benzene ring. The bands at 1268, 1160 and 1133 cm^{-1} were associated with C-O stretching vibration and C-H in-plane bending vibration of adsorbed phenolate [33,37,38]. Consequently, the conclusion could get that phenolate was obtained after the electroreductive dechlorination reaction of 2-chlorophenolate.

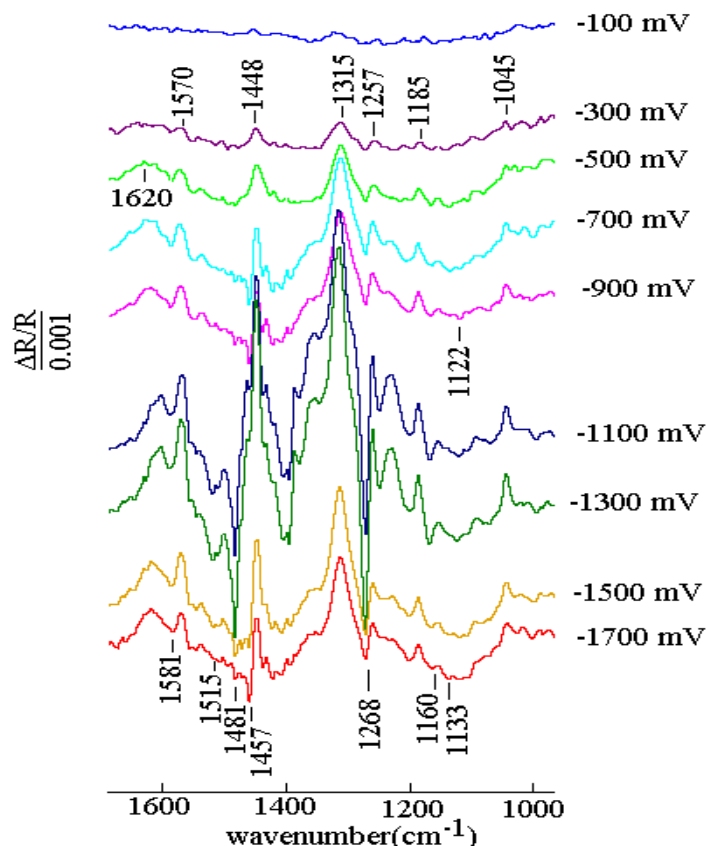


Figure 5. In situ FTIR spectra collected during electroreduction reaction of 2,3-DCP on Pd/Ag/Cu electrode.

When the potential stepped to -1500 mV, the intensities of the IR bands decreased gradually, there were two main reasons to explain the phenomenon: (1) hydrogen evolution reaction occurred and become the main reaction instead of electroreductive dechlorination reaction; (2) the final product phenolate desorbed from the surface of electrode with the spillover of hydrogen out of the thin film.

3.4 Theoretical calculate.

The BDE values and the length of C-Cl bonds of 2,3-DCP are compared and listed in Fig. 6. The BDE value of C2-Cl bond was greater than that of C3-Cl bond. It was well known that the bigger BDE value, the more difficult the corresponding bond was to break. So C2-Cl was a little more difficult to be eliminated than C3-Cl. This phenomenon in the adjacent bond strength was caused by

the oxy anionic substituent effect, and the presence of the donor group on benzene ring made C2-Cl bond stronger [39].

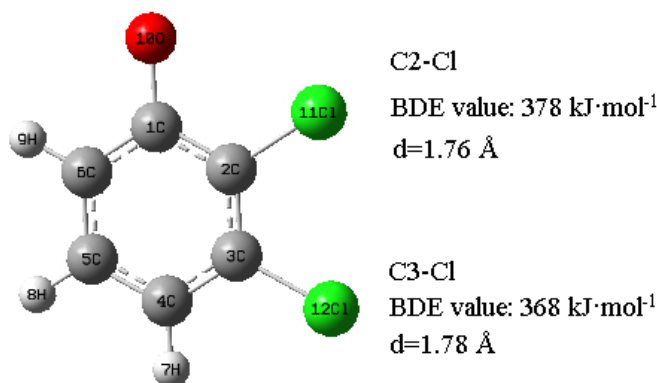
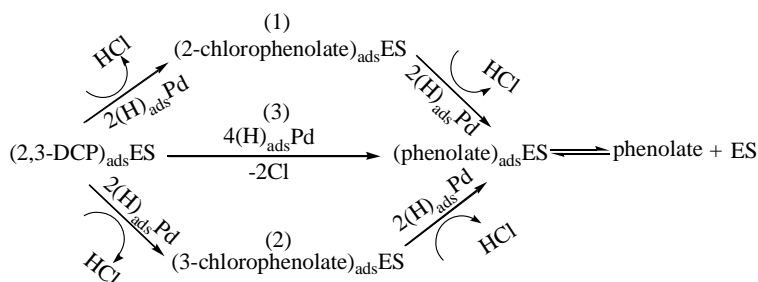


Figure 6. The BDE values and the length of C-Cl bonds of 2,3-DCP

To further demonstrate this, preparative electrolysis experiments of 2,3-DCP were performed on Pd/Ag/Cu, which was the most representative treatment method of wastewater [40]. The reaction was monitored and analyzed by high performance liquid chromatography (HPLC). It was found that the main intermediate product was 2-chlorophenolate with a small amount of 3-chlorophenolate, and the end product was phenolate without other compounds. According to the results of above analysis and literatures [41,42], the pathway for electroreductive dechlorination of 2,3-DCP on Pd/Ag/Cu electrode is illustrated in Scheme 1, where ES is the cathode surface of Pd/Ag/Cu electrode. Firstly, (H)_{ads}Pd was generated by reduction of water. Then C-Cl bonds broke by the reaction of adsorbed 2,3-DCP with (H)_{ads}Pd, and 2-chlorophenolate and 3-chlorophenolate were obtained, as shown in pathway (1) and (2). Finally, with electroreductive dechlorination reaction of the two chlorophenolates, the final product phenolate was obtained. With the pathway (3), phenolate could also be obtained with the cleavage of the bonds C2-Cl and C3-Cl directly. C3-Cl bond was easier to take off the benzene ring than C2-Cl bond, so 2-chlorophenolate was the main intermediate, and the electroreductive dechlorination reaction of 2,3-dichlorophenolate occurred on Pd/Ag/Cu electrode mainly according to the pathway (1).



Scheme 1. Mechanism of electroreductive dechlorination reaction of 2,3-DCP on Pd/Ag/Cu electrode. (ES is the electrode surface of Pd/Ag/Cu)

4. CONCLUSIONS

In summary, Ag dendrite-based Pd/Ag/Cu electrode was prepared by simple galvanic replacement reactions at room temperature. It was found that Pd/Ag/Cu electrode possessed high electrocatalytic activity toward 2,3-DCP electroreduction. C-Cl bonds was broken by the reaction of the adsorbed 2,3-DCP reacted with $(H)_{ads}Pd$ on the Pd/Ag/Cu electrode surface. The relative position of the chlorine atom on the benzene ring affected the electroductive behavior. At -300 mV, the electroreductive dechlorination of 2,3-DCP occurred and C3-Cl bond was broken, then the main intermediate 2-chlorophenolate was obtained, and the final product of 2,3-DCP electroreduction was phenolate.

ACKNOWLEDGMENTS

This work is supported by 973 national key basic research development program (2012CB722604) and Analysis and Testing Technology Project of Zhejiang province (2014C37038). The financial supports are gratefully acknowledged.

References

1. P.S. Majumder and S.K. Gupta, *Bioresour. Technol.*, 98 (2007) 118.
2. Y. Liu, F. Yang and P.L. Yue, G. Chen, *Water Res.*, 35 (2001) 1887.
3. J. Arana, E. Pulido Melian, V.M. Rodriguez Lopez, A. Pena Alonso, J.M. Dona Rodriguez, O. Gonzalez Diaz and J. Perez Pena, *J. Hazard. Mater.*, 146 (2007), 520.
4. F. Wang, Z.Q. Fan, X.H. Wu, M.C. Li and C.A. Ma, *Int. J. Electrochem. Sci.*, 10 (2015) 5101.
5. G. Chen, Z.Y. Wang and D.G. Xia, *Electrochim. Acta*, 50 (2004) 933.
6. Z.R. Sun, X.F. Wei, X. Hu, K. Wang and H.T. Shen, *Colloids and Surfaces A: Physicochem. Eng. Aspects*, 414 (2012) 314.
7. D.J. Guo and H.L. Li, *J. Colloid Interf. Sci.*, 286 (2005) 274.
8. V.Z. Radkevich, T.L. Senko, K. Wilson, L.M. Grishenko, A.N. Zaderko and V.Y. Diyuk, *Appl. Catal. A: Gen.*, 335 (2008) 241.
9. J.J. Shi and J.J. Zhu, *Electrochim. Acta*, 56 (2011) 6008.
10. P. Sangeetha, K. Shanthi, K.S.R. Rao, B. Viswanathan and P. Selvam, *Appl. Catal. A: Gen.*, 353 (2009) 160.
11. W.C. Ye, Y. Chen, F. Zhou, C.M. Wang and Y.M. Li, *J. Mater. Chem.*, 22 (2012) 18327.
12. X. Qin, H.C. Wang, X.S. Wang, Z.Y. Miao, Y.X. Fang, Q. Chen and X.G. Shao, *Electrochim. Acta*, 56 (2011) 3170.
13. A. Gutés, C. Carraro and R. Maboudian, *J. Am. Chem. Soc.*, 132 (2010) 1476.
14. J.F. Huang, S. Vongehr, S.C. Tang, H.M. Lu, J.C. Shen and X.K. Meng, *Langmuir*, 25 (2009) 11890.
15. M. Pera-Titus, V. García-Molina, M.A. Baños, J. Giménez and S. Esplugas, *Appl. Catal. B: Environ.*, 47 (2004) 219.
16. N. Oturan, M. Panizza and M.A. Oturan, *J. Phys. Chem. A*, 113 (2009) 10988.
17. M.S. Ureta-Zanartu, P. Bustos, M.C. Diez, M.L. Mora and C. Gutierrez, *Electrochim. Acta*, 46 (2001) 2545.
18. M. De Backer and F.X. Sauvage, *J. Electroanal. Chem.*, 602 (2007) 131.
19. G.A. Camara, R.B. de Lima and T. Iwasita, *J. Electroanal. Chem.*, 585 (2005) 128.
20. Q. Wang, G.Q. Sun, L.H. Jiang, Q. Xin, S.G. Sun, Y.X. Jiang, S.P. Chen, Z. Jusys and R.J. Behm,

- Phys. Chem. Chem. Phys.*, 9 (2007) 2686.
21. A.D. Becke, *Phys. Rev. A*, 38 (1988) 3098.
 22. A.D. Becke, *J. Chem. Phys.*, 97 (1992) 9173.
 23. A.D. Becke, *J. Chem. Phys.*, 98 (1993) 5648.
 24. C. Lee, W. Yang and R.G. Parr, *Phys. Rev. B*, 37 (1988) 785.
 25. J. Suegara, B.D. Lee, M.P. Espin, S. Nakai and M. Hosomi, *Chemosphere* 61 (2005) 341.
 26. R. Walsh, *Acc. Chem. Res.*, 14 (1981) 246.
 27. Y.Z. Lu and W. Chen, *J. Phys. Chem. C*, 114 (2010) 21190.
 28. Y. Sun, Z. Tao, J. Chen, T. Herricks and Y. Xia, *J. Am. Chem. Soc.*, 126 (2004) 5940.
 29. C.A. Ma, Hao, Ma, Y.H., Xu, Y.Q. Chu and F.M. Zhao, *Electrochem. Commun.*, 11 (2009) 2133.
 30. C.C. Hu and T.C. Wen, *Electrochim. Acta*, 40 (1995) 495.
 31. D.D. Macdonald, *J. Electrochem. Soc.*, 121 (1974) 651.
 32. W.C. Wu, L.F. Liao, C.F. Lien and J.L. Lin, *Phys. Chem. Chem. Phys.*, 3 (2001) 4456.
 33. R. Chetty and P.A. Christensen, B.T. Golding, K. Scott, *Appl. Catal. A: Gen.*, 271 (2004) 185.
 34. M.C. Li, D.D. Bao and C.A. Ma, *Electrochim. Acta*, 56 (2011) 4100.
 35. J. Bandara, J.A. Mielczarski, J. Kiwi, *Appl. Catal. B: Gen.*, 34 (2001), 307.
 36. J.M. Delgado, A. Berná, J.M. Orts, A. Rodes and J.M. Feliu, *J. Phys. Chem. C*, 111 (2007) 9943.
 37. R. Chetty and P.A. Christensen, B.T. Golding, *Chem. Commun.*, (2003) 984.
 38. R.D. Webster, *Electrochem. Commun.*, 5, (2003) 6.
 39. M. L. Steigerwald, W.A. Goddard III and D.A. Evans, *J. Am. Chem. Soc.*, 101 (1979) 1994.
 40. C.Y. Yun, D.G. Kim, W.Y. Kim, D.J. Son, D. Chang, J.H. Kim, Y.S. Bae, H.S. Bae, Y. Sunwoo, M.S. Kwak and K.H. Hong, *Int. J. Electrochem. Sci.*, 9 (2014) 1522.
 41. C.Y. Cui, X. Quan, H.T. Yu, and Y.H. Han, *Appl. Catal. B: Environ.*, 80 (2008) 122.
 42. G. Chen, Z.Y. Wang, T. Yang, D.D. Huang and D.G. Xia, *J. Phys. Chem. B*, 110 (2006) 4863.